Nonlinear multiple passage effects on optical imaging of an absorption inhomogeneity in turbid media

M. Xu, W. Cai and R. R. Alfano

Institute for Ultrafast Spectroscopy and Lasers,
New York State Center of Advanced Technology for Ultrafast Photonic Materials and Applications,
and Department of Physics,
The City College and Graduate Center of City University of New York, New York, NY 10031

ABSTRACT

We report on the effect of the nonlinear multiple passage on optical imaging of an absorption inhomogeneity of finite size deep inside a turbid medium based on a cumulant solution to radiative transfer. An analytical expression for the nonlinear correction factor is derived. Comparison to Monte Carlo simulations reveals an excellent agreement. The implication on optical imaging is discussed.

Keywords: nonlinear correction, multiple passage, radiative transfer, optical imaging

1. INTRODUCTION

The principle of optical imaging of turbid media (such as tissues) is to locate and reconstruct the optical properties (absorption and scattering coefficients) of embedded inhomogeneities (such as tumor) in the hope of identification by inverting the difference in time-resolved or frequency-modulated photon transmittance due to the presence of the inhomogeneities through either iterative or noniterative methods. The key quantity involved is the weight function which quantifies the influence on the detected signal due to the change of the optical parameters of the medium. The diffusion approximation to radiative transfer provides an adequate model for the weight function (or Jacobian) for a small and weak absorption inhomogeneity far away from both the source and the detector. However, the weight function predicted by the linear perturbation approaches is no longer valid when the absorption strength is not small.[1] This can be attributed to the multiple passage of a photon through one single abnormal site.

The change of the light intensity ΔI at the detector $\mathbf{r}_d$ due to the presence of an absorption site at $\mathbf{r}$ from a modulated point source at $\mathbf{r}_s$ is expressed as

$$\Delta I = -\delta\mu_a V G(\mathbf{r}_d, \omega|\mathbf{r}) G(\mathbf{r}, \omega|\mathbf{r}_s) \tag{1}$$

to the first order of Born approximation where $\delta\mu_a$ is the excess absorption of the absorption site whose volume is V, ω is the modulation frequency of light, and G is the propagator of photon migration in the background medium. Here, the Green's function $G(\mathbf{r}_2, \omega|\mathbf{r}_1)$, in general, depends on the detail of light scattering inside the medium, and the incident and outgoing directions of light.

When the absorption strength is not small ($\delta\mu_a V \not\ll 1$), photon loss due to multiple passage of the absorption site is appreciable and can not be ignored. The expression for ΔI in Eq. (1) needs to be modified to include the contributions from multiple visits of the site by the photon. Fig. (1) illustrates the most important correction (a "self-energy" correction) which takes into account the repeated visits made by a photon to the site up to an infinite times.

Further author information: (Send correspondence to M. Xu)
M. Xu: Email: minxu@sci.ccny.cuny.edu

Photon Migration and Diffuse-Light Imaging, David A. Boas, Editor,
Proceedings of SPIE-OSA Biomedical Optics, SPIE Vol. 5138 (2003)

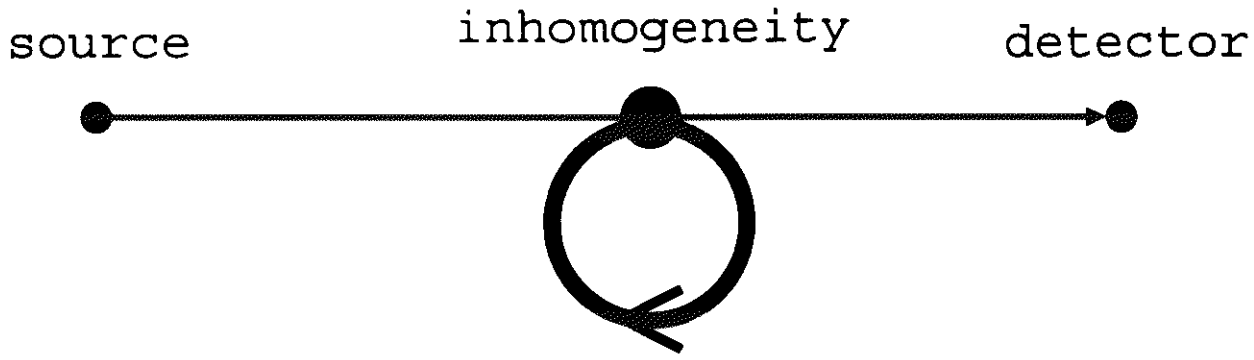

Figure 1. Self-energy correction to the multiple passage effect on light absorption.

Assuming that the center of the absorption site is located at $\bar{\mathbf{r}}$ and far away from both the source and the detector, the change of the detected light, ΔI, is now given by

$$\begin{aligned} \Delta I &= -G(\mathbf{r}_d, \omega|\mathbf{r}) V\delta\mu_a(\mathbf{r}) \sum_{n=0}^{\infty} \left(-\bar{N}_{\text{self}}(\omega; R) V\delta\mu_a(\bar{\mathbf{r}})\right)^n G(\bar{\mathbf{r}}, \omega|\mathbf{r}_s) \\ &= -G(\mathbf{r}_d, \omega|\mathbf{r}) \frac{V\delta\mu_a(\bar{\mathbf{r}})}{1 + \bar{N}_{\text{self}}(\omega; R) V\delta\mu_a(\bar{\mathbf{r}})} G(\mathbf{r}, \omega|\mathbf{r}_s) \end{aligned} \tag{2}$$

where

$$\bar{N}_{\text{self}}(\omega; R) = \frac{1}{V^2} \int_V \int_V G(\mathbf{r}_2, \omega|\mathbf{r}_1) d^3\mathbf{r}_2 d^3\mathbf{r}_1 \tag{3}$$

is the self-propagator which describes the probability that a photon revisits the volume V of size R. Here $G(\mathbf{r}_d, \omega|\mathbf{r})$ and $G(\mathbf{r}, \omega|\mathbf{r}_s)$ are well modelled by the center-moved diffusion model as long as the separations $|\mathbf{r}_d - \mathbf{r}|$, $|\mathbf{r}_s - \mathbf{r}| \gg l_t$ where l_t is the transport mean free path of light in the medium.[2] However, the diffusion Green's function can not be used in Eq. (3) to evaluate $\bar{N}_{\text{self}}(\omega; R)$ where $\mathbf{r}_1$ is in the proximity of $\mathbf{r}_2$. By comparing Eq. (2) to Eq. (1), the nonlinear multiple passgage effect of an absorption site can be summarized by the nonlinear correction factor $\left[1 + \bar{N}_{\text{self}}(\omega; R) V\delta\mu_a(\bar{\mathbf{r}})\right]^{-1}$. This factor serves as a universal measure of the nonlinear multiple passage effect as long as the absorption site is far away from both the source and the detector and its size is much smaller than its distance to both the source and the detector.

In this article, we will derive an analytical expression for the self-propagator to understand the nonlinear multiple passage effect on light absorption using our cumulant solution to radiative transfer. The nonlinear correction factor $\left[1 + \bar{N}_{\text{self}}(\omega; R) V\delta\mu_a(\mathbf{r})\right]^{-1}$ of our result is shown to be in an excellent agreement with the Monte Carlo simulations for continuous wave light.

2. THEORY

To take into account the higher order contributions from the absorption inhomogeneity, the behavior of the photon migration in a short distance must be considered. Although the photon distribution is almost isotropic at an absorption site deep inside the medium, the diffusion approximation is still not appropriate here. The separation between the two points $\mathbf{r}_1$ and $\mathbf{r}_2$ within the volume in Eq. (3) is small. The photon propagator $N(\mathbf{r}_2, t|\mathbf{r}_1, \mathbf{s})$, which 23 is the probability that a photon propagates

from position $\mathbf{r}_1$ with propagation direction $\mathbf{s}$ to position $\mathbf{r}_2$ in time t, when $\mathbf{r}_2$ is in the proximity of $\mathbf{r}_1$, is governed by the radiative transfer equation rather than the diffusion equation.

Recently we have shown that the propagation of photon inside a turbid medium (the radiative transfer equation) can be solved analytically using a cumulant expansion of the photon distribution function.[3] The propagation of photon was found to transform from an initial ballistic motion at early time and then gradually to a center-adjusted diffusion at later time. The propagator of photon density (the Green's function) in an infinite uniform medium is given by[4]

$$N(\mathbf{r}, t|\mathbf{r}_0, \mathbf{s}_0) = \frac{1}{[4\pi D(t)t]^{3/2}} \exp\left[-\frac{(\mathbf{r} - \mathbf{r}_0 - \mathbf{s}_0\Delta(t))^2}{4D(t)t} - \mu_a t\right] \tag{4}$$

ignoring the small difference in the diffusion coefficient along different directions where the absorption coefficient is μ_a, the time-dependent diffusion coefficient is

$$D(t) = \frac{l_t^2}{3t}\left\{\frac{ct}{l_t} - [1 - \exp(-ct/l_t)] - \frac{1}{2}[1 - \exp(-ct/l_t)]^2\right\} \tag{5}$$

and

$$\Delta(t) = l_t[1 - \exp(-ct/l_t)] \tag{6}$$

is the average center of photons which moves with speed c initially and approaches the transport mean free path l_t in the long time limit. The Green's function for parallel geometries can be obtained by the method of image sources.[5]

2.1. Propagator of an isotropic point source

Let's now consider the propagator $N(\mathbf{r}, t|\mathbf{r}_0, \mathbf{s}_0)$ at the inhomogeneity site $\mathbf{r}_0 = \mathbf{0}$ (the origin of space) deep inside the medium. The photon distribution at $\mathbf{r}_0$ is almost isotropic but is *anisotropic* scattering. The effective propagator can then be obtained by averaging (4) over the propagation direction $\mathbf{s}_0$ of light over the 4π solid angle, and is given by [see Appendix A]

$$\begin{aligned} N_{\text{eff}}(r, t) &= \frac{1}{4\pi}\int d^2\mathbf{s}_0 N(\mathbf{r}, t|\mathbf{r}_0, \mathbf{s}_0) = \frac{\exp(-\mu_a t)}{(4\pi)^{3/2}(D(t)t)^{1/2} r\Delta(t)} \\ &\times \left\{\exp\left[-\frac{(r - \Delta(t))^2}{4D(t)t}\right] - \exp\left[-\frac{(r + \Delta(t))^2}{4D(t)t}\right]\right\}. \end{aligned} \tag{7}$$

This reduces to

$$N_{\text{eff}}(r, t) = \frac{\exp(-\mu_a t)}{4\pi r^2}\delta(r - ct), \quad \text{for } t \to 0^+ \tag{8}$$

and

$$N_{\text{eff}}(r, t) = \frac{\exp(-\mu_a t)}{(4\pi)^{3/2}(D_\infty t)^{1/2} r l_t}\left\{\exp\left[-\frac{(r - l_t)^2}{4D_\infty t}\right] - \exp\left[-\frac{(r + l_t)^2}{4D_\infty t}\right]\right\}, \quad \text{for t} \gg 1 \tag{9}$$

in early and late time limits where $D_\infty \equiv l_t c/3$.

The temporal Fourier transforms of the asymptotic equations (8) and (9) are given by

$$N_{\text{eff}}(\mathbf{r}, \omega) = \frac{1}{4\pi r^2 c}\exp\left[(i\omega - \mu_a)\frac{r}{c}\right] \tag{10}$$

and

$$N_{\text{eff}}(\mathbf{r},\omega) = \frac{1}{8\pi D r \kappa l_t}\left[\exp(-\kappa\,|r-l_t|) - \exp(-\kappa(r+l_t))\right] \tag{11}$$

respectively, where $\kappa \equiv \sqrt{3(\mu_a - i\omega)/l_t c}$ whose sign is chosen with a nonnegative real part. In the limit of small $\kappa \ll 1$, Eq. (11) simplifies to

$$\lim_{\kappa\to 0} N_{\text{eff}}(\mathbf{r},\omega) = \begin{cases} \frac{1}{4\pi D_\infty l_t} & r < l_t \\ \frac{1}{4\pi D_\infty r} & r \geq l_t \end{cases}. \tag{12}$$

This is the case, for example, that a continuous wave propagates in a nonabsorbing medium. The errornous divergence at the zero separation in the diffuse Green's function

$$G(r,\omega) = \frac{\exp(-\kappa r)}{4\pi D_\infty r} \tag{13}$$

is removed in our formulation of the propagation of an isotropic point source.

The asymptotic equation (11) from the late time limit provides a good approximation for $N_{\text{eff}}(r,\omega)$ when $r > l_t$ [see Fig. (2)]. The contribution to $N_{\text{eff}}(r,\omega)$ when $r < l_t$ is from either ballistic or diffusive photons, hence an improvement to Eq. (10) can be made

$$N_{\text{eff}}(r,\omega) \simeq \frac{1}{4\pi r^2 c}\exp\left[(i\omega-\mu_a)\frac{r}{c}\right] + \frac{\exp(-\kappa l_t)}{4\pi D_\infty r \kappa l_t}\sinh(\kappa r), \quad r < l_t \tag{14}$$

to include the contribution from diffusive photons. The effective propagator in temporal Fourier space $N_{\text{eff}}(r,\omega=0)$ and its asymptotic behaviors (10), (11) and (14) are shown in Fig. (2). The diffusion Green's function has a huge error for small r.

2.2. Self propagator for a finite volume

For an absorption site of a finite volume V deep inside the medium, say a sphere of radius $R \ll L$ where L is the dimension of the medium, the self-propagator $N_{\text{self}}(t;R)$ for this volume which denotes a photon revisits the site in time t is written as:

$$\begin{aligned} N_{\text{self}}(t;R) &= \frac{1}{V^2}\int_V\int_V N_{\text{eff}}(|\mathbf{r}_2-\mathbf{r}_1|,t)d^3\mathbf{r}_1 d^3\mathbf{r}_2 \\ &= \frac{1}{V}\int_0^{2R} N_{\text{eff}}(r,t)\gamma_0(r)4\pi r^2 dr \end{aligned} \tag{15}$$

where

$$\gamma_0(r) = 1 - \frac{3r}{4R} + \frac{1}{16}\left(\frac{r}{R}\right)^3 \tag{16}$$

is the characteristic function for a uniform sphere.[6-8] This characteristic function has a form of

$$\gamma_0(r) = 1 - (S/4V)r + \ldots \tag{17}$$

for an arbitrary particle where S is the surface area of the particle. This self propagator (15) for a finite volume is quite different from the self-propagator of a point, obtained by setting $r = 0$ in (4) or (7), i.e.,

$$N_{\text{self}}(0,t) = \frac{\exp(-\mu_a t)}{(4\pi D(t)t)^{3/2}}\exp\left[-\frac{\Delta(t)^2}{D(t)t}\right], \quad (t>0). \tag{18}$$

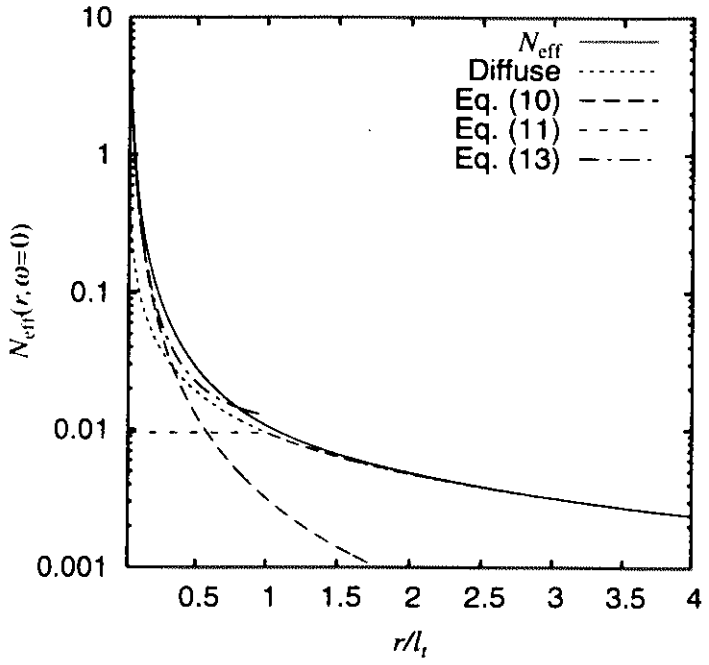

Figure 2. The effective propagator in temporal Fourier space $N_{\rm eff}(r,\omega=0)$ for photon migration in a nonabsorbing medium. Its approximations by (14) when $r < l_t$ and by Eq. (11) when $r > l_t$ are also plotted. The diffusion Green's function has a huge error for small r.

See Fig. (3). This difference comes from the fact that Eq. (15) includes the contribution from the ballistic motion of the photon when the photon flies across the site while Eq. (18) does not contain this effect. The former manifests itself in Fig. (3a) as the linear decay of $N_{\rm seff}(t;R)V$ in the form of $\gamma_0(ct)$ near the origin.

The self-propagator in temporal Fourier space is thus obtained by a temporal Fourier transform of (15):

$$\begin{aligned}\bar{N}_{\rm self}(\omega;R) &= \int_{0^+}^{+\infty} \bar{N}_{\rm self}(t;R)\exp(i\omega t)dt \\ &= \frac{1}{V}\int_0^{2R} dr\gamma_0(r)4\pi r^2 \int_0^{+\infty} dt N_{\rm eff}(r,t)\exp(i\omega t) \\ &= \frac{1}{V}\int_0^{2R} N_{\rm eff}(r,\omega)\gamma_0(r)4\pi r^2 dr.\end{aligned} \tag{19}$$

The lower limit of integration is 0^+, emphasizing that $t=0$ should be excluded from integration. Note $\lim_{t\to 0^+}\bar{N}_{\rm eff}(r,t)=0$ for our cumulant photon density function. This is not the case for the diffusion Green's function. A numerical quadrature is generally required to compute this self propagator (19). A crude estimation of $\bar{N}_{\rm self}(\omega;R)$ can be obtained from the asymptotic behavior (11) and (14) of $N_{\rm eff}(r,\omega)$, i.e.,

$$\begin{aligned}\bar{N}_{\rm seff}(\omega;R) \simeq\ & \frac{1}{V}\int_0^{\min(2R,l_t)} \frac{1}{4\pi r^2 c}\exp\left[(i\omega-\mu_a)\frac{r}{c}\right]\gamma_0(r)4\pi r^2 dr \\ & +\frac{1}{V}\int_0^{2R}\frac{1}{8\pi D_\infty r\kappa l_t}\left[\exp(-\kappa|r-l_t|)-\exp(-\kappa(r+l_t))\right]\gamma_0(r)4\pi r^2 dr.\end{aligned} \tag{20}$$

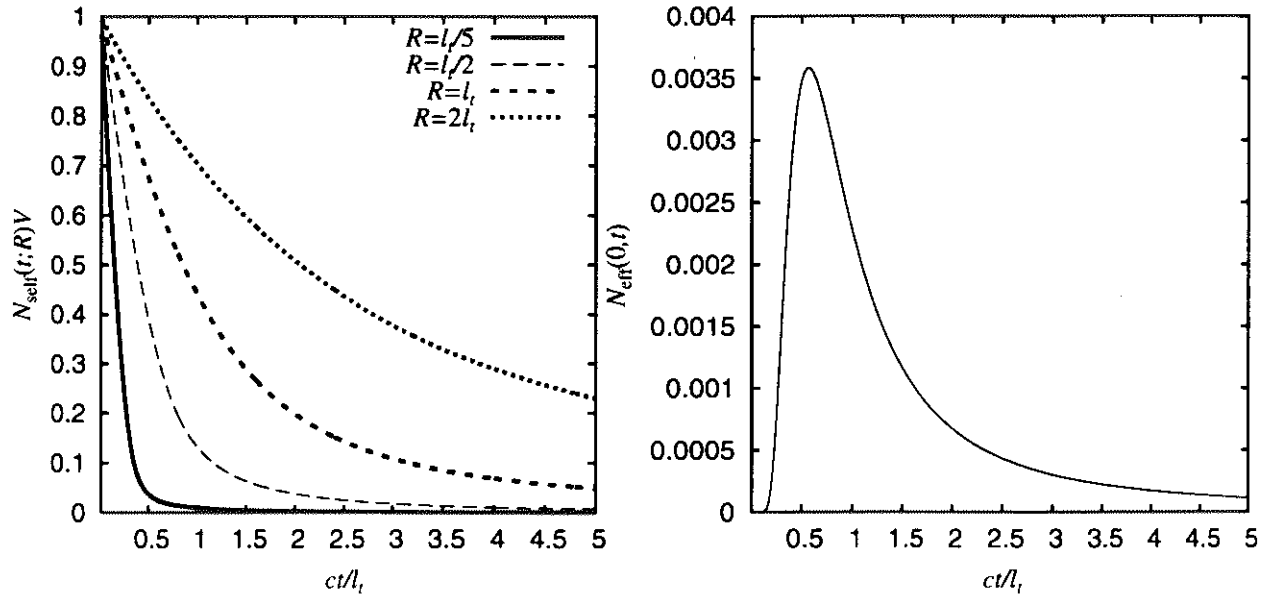

(a) (b)

Figure 3. The self-propagators for a finite volume and a point: (a) $N_{\text{self}}(t; R)$ and (b) $N_{\text{eff}}(\mathbf{0}, t)$.

This reduces to

$$\bar{N}_{\text{self}}(\omega = 0; R) = \frac{1}{V} \begin{cases} \frac{3R}{4c} + \frac{R^3}{l_t^2 c} & R \le l_t/2 \\ \frac{384R^5 + 160l_t^2R^3 - 60l_t^3R^2 + 3l_t^5}{320R^3 l_t c} & R > l_t/2 \end{cases} \tag{21}$$

for a continuous wave propagating inside a nonabsorbing medium ($\omega = \mu_a = \kappa = 0$). This estimation turns out to be amazingly good. Fig. (4) plots $\bar{N}_{\text{self}}(\omega = 0; R)$ from numerical quadrature and the crude estimation (21).

3. RESULTS AND DISCUSSION

The multiple passage effect due to the absorption site can now be computed using the self-propagator Eq. (19) derived here. For large sites, the self-propagator $\bar{N}_{\text{self}}(\omega = 0; R)$ increases inverse proportional to its size ($\bar{N}_{\text{self}} \propto R^{-1}$) from Eq. (21); hence the nonlinear correction factor has a form of

$$\frac{1}{1 + \bar{N}_{\text{self}}(\omega; R) V \delta\mu_a(\bar{\mathbf{r}})} \simeq \left(1 + \frac{6\delta\mu_a}{5l_t c} R^2\right)^{-1}. \tag{22}$$

dependent on the area of the absorption site for large R.

Monte Carlo methods have been extensively used in simulation of photon migration.[9,10] We perform Monte Carlo simulations on a uniform nonabsorbing and isotropic scattering slab (the anisotropic factor of scattering $g = 0$). The units of length of time are chosen such that the mean scattering length $l_s = 1/\mu_s = 1$ and the speed of light $c = 1$. The transport mean free path is hence $l_t = 1$ and the thickness of the slab is assumed $L = 80l_t$. An absorption spherical site is located at the center of the slab $(0, 0, L/2)$ with radius R whose absorption and scattering coefficients are $\mu_{a,2} = \delta\mu_a = 0.01$ and

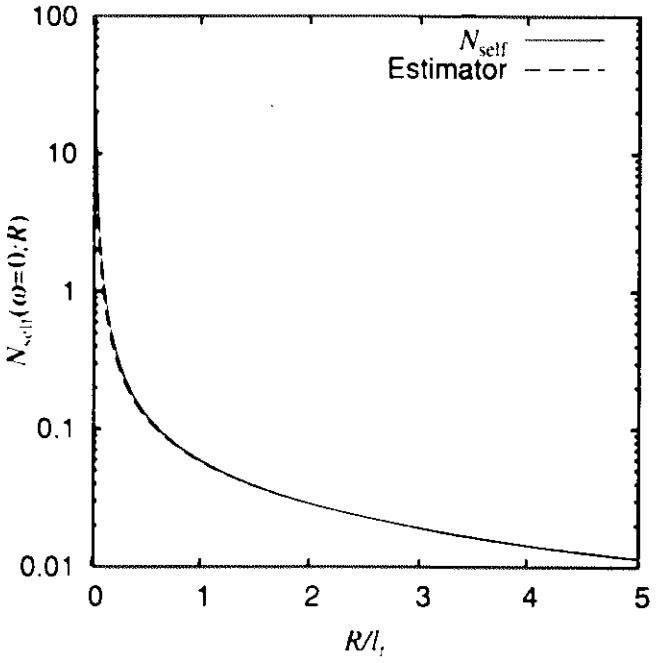

Figure 4. The self propagator $N_{self}(\omega = 0; R)$ and its estimator. The diffusion self-propagator for continuous waves is also plotted.

$\mu_{s,2} = \mu_s$ respectively. The photon is incident at the origin on the left boundary of the slab $z = 0$ in the normal direction of the surface. Each photon is traced until it escapes the slab through either the left or the right boundary. The correlated sampling is used in simulation to reduce variance. A single simulation is used to compute the emitted photon density I_0 for the uniform background (nonabsorption slab) and I for the slab with the absorption site present.

The nonlinear correction factor $[1 + \bar{N}_{self}(\omega; R)V\delta\mu_a(\bar{\mathbf{r}})]^{-1}$ in Eq. (22) can be extracted from the change of the detected light intensity due to the presence of the absorption site in Monte Carlo simulations according to Eq. (2). Fig. (5) plots the theoretical nonlinear correction factor and that from Monte Carlo simulations. "Back" and "Forward" denote the cases where light emits from the left ($z = 0$) and the right ($z = L$) boundaries, respectively. The agreement between our theoretical result and Monte Carlo simulations is excellent except for extremely small sizes of inhomogeneities.

Figs. (6) and (7) plot the nonlinear correction factor versus the variation of the modulation frequency of light for a fixed absorption strength and versus the size of the absorption site with a fixed modulation frequency of light respectively. With the increase of the modulation frequency of light, the nonlinear correction becomes less accentuated. The dependence on the size of the inhomogeneity is no longer monotonic for modulated light while the nonlinear correction factor decreases monotonically with the increase of the size for continuous wave light. The phase delay is in the order of a few degrees in the cases investigated.

The typical value of the absorption coefficient of human tissues is around 0.001ps^{-1} while the scattering coefficient is about 1ps^{-1}. Hence the absorption and scattering ratio is in the order of 0.001. This should be compared to our results listed here where the corresponding ratio is 0.01 and one order of magnitude stronger. The nonlinear correction factor for absorption inhomogeneities such as tumors in human tissues is not appreciable unless the size of the inhomogeneity is $R \sim 5l_t$ or larger.

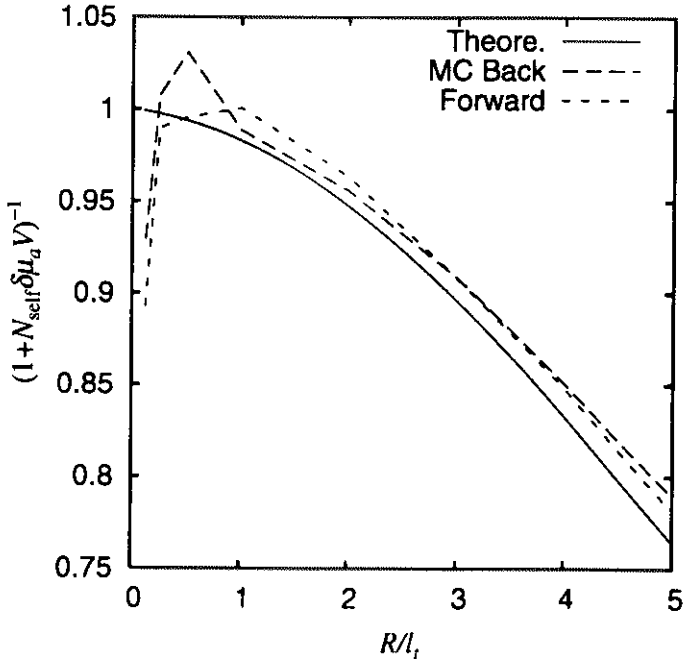

Figure 5. The nonlinear correction factor from the theoretical self-propagator Eq. (19) and Monte Carlo simulations. "Back" and "Forward" denote light emitting from the left (z=0)and the right ($z = L$) boundaries. The excess absorption is $\delta\mu_a = 0.01$.

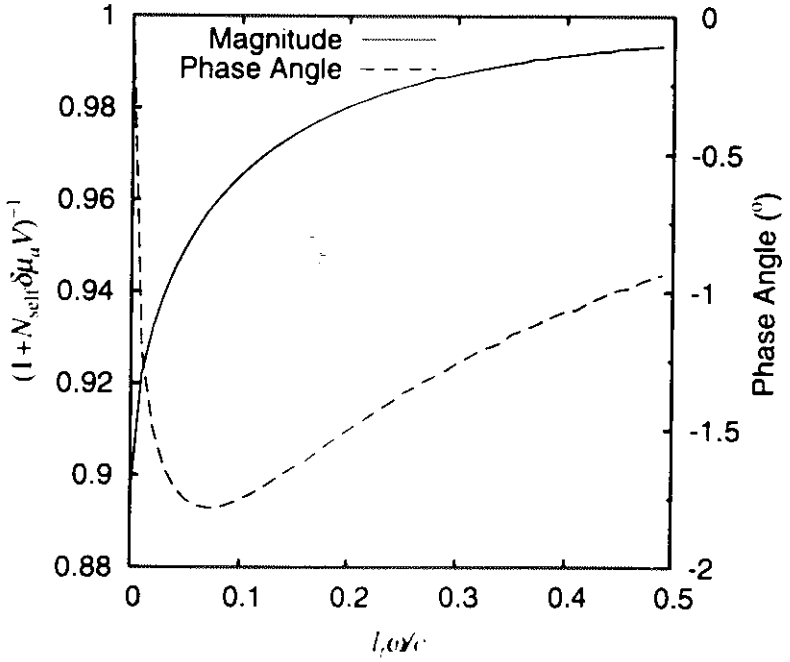

Figure 6. The nonlinear correction factor versus the variation of the modulation frequency of light. The size of the absorption sphere is $R = 3l_t$. The excess absorption 0.01.

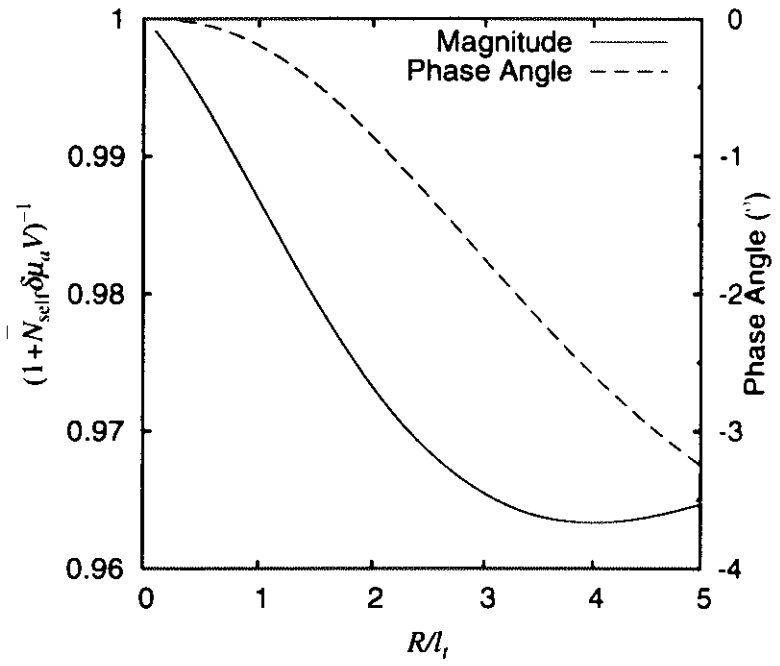

Figure 7. The nonlinear correction factor versus the variation of the size of the absorption site. The modulation frequency of light is $\omega = 0.1$. The excess absorption is $\delta\mu_a = 0.01$.

In conclusion, we have derived an analytical expression for the nonlinear correction factor which agrees well with Monte Carlo simulations. The effect of the nonlinear multiple passage of an absorption site on optical imaging only becomes appreciable when the size of the inhomogeneity is $5l_t$ or larger for human tissues.

APPENDIX A. DERIVATION OF $N_{\mathrm{EFF}}(R,T)$

The spatial Fourier transform of (4) is given by

$$N(\mathbf{k},t|\mathbf{r}_0,\mathbf{s}_0) = \int d^3\mathbf{r}\exp(-i\mathbf{k}\cdot\mathbf{r})N(\mathbf{r},t|\mathbf{r}_0,\mathbf{s}_0) = \exp\left(-k^2D(t)t - \mu_a t - i\mathbf{k}\cdot\mathbf{s}_0\Delta(t)\right). \quad (23)$$

Hence, the effective propagator in spatial Fourier space at $\mathbf{r}_0$ is expressed as

$$N_{\mathrm{eff}}(\mathbf{k},t) = \frac{1}{4\pi}\int d^2\mathbf{s}_0 N(\mathbf{k},t|\mathbf{r}_0,\mathbf{s}_0) = \exp\left(-k^2D(t)t - \mu_a t\right)\frac{\sin(k\Delta(t))}{k\Delta(t)} \quad (24)$$

by averaging (23) over the propagation direction $\mathbf{s}_0$ of light over the 4π solid angle. The effective propagator in real space is then obtained by an inverse spatial Fourier transform of (24):

$$\begin{aligned} N_{\mathrm{eff}}(\mathbf{r},t) &= \int \frac{d^3\mathbf{k}}{(2\pi)^3}\exp(i\mathbf{k}\cdot\mathbf{r})\exp\left(-k^2D(t)t - \mu_a t\right)\frac{\sin(k\Delta(t))}{k\Delta(t)} \\ &= \frac{\exp(-\mu_a t)}{(4\pi)^{3/2}(D(t)t)^{1/2}r\Delta(t)}\left\{\exp\left[-\frac{(r-\Delta(t))^2}{4D(t)t}\right] - \exp\left[-\frac{(r+\Delta(t))^2}{4D(t)t}\right]\right\} \\ &= \frac{2\exp(-\mu_a t)}{(4\pi)^{3/2}(D(t)t)^{1/2}r\Delta(t)}\exp\left[-\frac{r^2+\Delta(t)^2}{4D(t)t}\right]\sinh\frac{r\Delta(t)}{2D(t)t}. \end{aligned} \quad (25)$$

ACKNOWLEDGMENTS

This work is partly supported by US Army Medical Research and Materiels Command, NASA IRA, and CUNY organized research programs. One of the authors (M. Xu) thanks the support by the Department of Army (Grant# DAMD17-02-1-0516). The U. S. Army Medical Research Acquisition Activity, 820 Chandler Street, Fort Detrick MD 21702-5014 is the awarding and administering acquisition office.

REFERENCES

1. S. Carraresi, T. S. M. Shatir, F. Martelli, and G. Zaccanti, "Accuracy of a perturbation model to predict the effect of scattering and absorbing inhomogeneities on photon migration," *Appl. Opt.* **40**, pp. 4622–4632, Sept. 2001.
2. M. Xu, W. Cai, M. Lax, and R. R. Alfano, "A transport model for optical tomography in turbid media," in *Signal Recovery and Synthesis*, OSA, 2001.
3. W. Cai, M. Lax, and R. R. Alfano, "Cumulant solution of the elastic Boltzmann transport equation in an infinite uniform medium," *Phys. Rev. E* **61**(4-A), pp. 3871–3876, 2000.
4. M. Xu, W. Cai, M. Lax, and R. R. Alfano, "A photon transport forward model for imaging in turbid media," *Opt. Lett.* **26**(14), pp. 1066–1068, 2001.
5. M. Xu, W. Cai, M. Lax, and R. R. Alfano, "Photon migration in turbid media using a cumulant approximation to radiative transfer," *Phys. Rev. E* **65**, p. 066609, 2002.
6. G. Porod, "Die röntgenkleinwinkelstreuung von dichtgepackten kolloiden systemen i," *Kolloid-Z.* **124**, pp. 83–114, 1951.
7. G. Porod, "Die röntgenkleinwinkelstreuung von dichtgepackten kolloiden systemen ii," *Kolloid-Z.* **125**, pp. 51–57, 109–122, 1952.
8. A. Guinier, G. Fournet, C. B. Walker, and K. L.Yudowitch, *Small-angle scattering of X-rays*, John Wiley & Sons, New York, 1955.
9. A. Sassaroli, C. Blumetti, F. Martelli, L. Alianelli, D. Contini, A. Ismaelli, and G. Zaccanti, "Monte Carlo procedure for investigating light propagation and imaging of highly scattering media," *Appl. Opt.* **37**, pp. 7392–7400, Nov. 1998.
10. M. Testorf, U. sterberg, B. Pogue, and K. Paulsen, "Sampling of time- and frequency-domain signals in monte carlo simulations of photon migration," *Appl. Opt.* **38**, pp. 236–245, January 1999.